

## Supporting Information

### **Finding the Most Catalytically Active Platinum Clusters With Low Atomicity\*\***

*Takane Imaoka, Hirokazu Kitazawa, Wang-Jae Chun, and Kimihisa Yamamoto\**

anie\_201504473\_sm\_miscellaneous\_information.pdf

## Experimental

**Materials.** Fourth-generation phenylazomethine dendrimers with a triphenylmethane (**DPAG4-TPM**) or pyridyl-triphenylmethane (**DPAG4-PyTPM**) core were synthesized. Preparations of all platinum clusters (Pt<sub>13</sub>–Pt<sub>20</sub>) through the chemical reduction of PtCl<sub>4</sub> in **DPAG4-TPM** were carried out as previously reported with different [PtCl<sub>4</sub>]/[**DPAG4-PyTPM**] stoichiometries.<sup>[1]</sup> The Pt<sub>12</sub> cluster was synthesized as previously reported.<sup>[1]</sup> Polyamidoamine dendrimer (**PAMAM G4-OH**) by Dendritech Inc. was purchased from Aldrich. **PAMAM G4-OH** was also employed for the synthesis of platinum clusters similar to the previous report.<sup>[2]</sup> To the solution of **PAMAM G4-OH** dissolved in ultrapure water ( $3.0 \times 10^{-6}$  mol L<sup>-1</sup>), K<sub>2</sub>PtCl<sub>4</sub> ( $3.0 \times 10^{-3}$  mol L<sup>-1</sup>) in water was added. After the equilibration for 48 hours at room temperature, a reducing agent NaBH<sub>4</sub> in water was added and stirred for 5 hours.

**STEM observation.** HAADF-STEM images were obtained using a standard transmission electron microscope (Jeol, JEM-2100F) or aberration-corrected TEM (Jeol, ARM-200F). All the cluster samples for STEM observations were supported on graphene as follows. High surface area (3 nm thickness) graphene powder (Alliance Biosystems, Inc.) was added to a resulting solution of the as-synthesized clusters. The amount of graphene was adjusted to 1.0 wt% of the platinum loaded on the carbon materials. The suspensions were then vigorously stirred for 1 min. Each of the carbon-supported platinum clusters was then deposited on an elastic carbon film with a Cu mesh (Nisshin EM Co.) followed by vacuum drying at 40 °C overnight.

**XAFS data acquisition.** XAFS was measured in the transmission mode at the BL9C and BL12C beamlines at the Photon Factory (KEK-IMSS), or in the fluorescence mode at the BL01B1 beamline at Spring-8 (JASRI) for *in situ* electrochemical measurements. Each synchrotron radiation from the storage ring was monochromatized with Si(111)

channel-cut crystals. The angle of the monochromator was calibrated using Pt foil. For transmission mode, ionization chambers filled with 15% Ar-85% N<sub>2</sub> mixed gas and 100% Ar were used as detectors to monitor the incident ( $I_0$ ) and transmitted X-rays ( $I$ ), respectively. For the fluorescence mode, a 19-element Ge solid-state detector was employed. The angle of the monochromator was calibrated using Pt foil. All the transmission measurements were conducted at 30 K while *in situ* measurements were obtained at room temperature. XAFS analyses were conducted using REX2000 software (Rigaku Co., Japan) as previously reported.<sup>[1]</sup> Backscattering phase shifts and amplitudes for Pt-Pt were extracted from Pt foil as a standard compound.

**Electrochemical measurements.** Electrochemical measurements were performed using a multipurpose electrochemical workstation (ALS-750b, CH Instruments). A glassy carbon disk electrode (6.0 mm diameter) was used as the working electrode. The electrode surface was polished with diamond and alumina paste, and then rinsed in methanol with ultrasonication prior to use. An Ag/AgCl electrode in 3 mol L<sup>-1</sup> NaCl<sub>aq</sub> and a platinum coil were used as the quasi-reference and counter electrodes, respectively. Cyclic voltammetry (CV) and RDV measurements were conducted in an aqueous HClO<sub>4</sub> solution (0.1 mol L<sup>-1</sup>), which was thoroughly bubbled with O<sub>2</sub> or N<sub>2</sub> gas prior to the measurements. During the measurements, the atmospheric conditions were kept constant with flowing O<sub>2</sub> or N<sub>2</sub> gas. For each cluster sample, the as prepared solution was cast on the electrode and then dried under vacuum. In the case of **PAMAM G4-OH**, equal amount of methanol was added to the as prepared solution before the cast. The variation in the amount of solution was 1–10 μL. The weight of the platinum element on the electrode was calculated from the concentration and volume used for the casting. The kinetic limiting current density was calculated using the Koutecky-Levich equation, as previously reported.<sup>[3]</sup>

**DFT calculations.** All the DFT calculations were performed using a DMol<sup>3</sup> module<sup>[4]</sup> within Material Studio 6.0 (Accelrys). The GGA-RPBE functional for the exchange and correlation was used. The DNP 3.5 (double numerical and polarization basis set provided with the Material Studio) was employed as the basis set. The preset values defined as the “fine” option were used for the integration accuracy, SCF tolerance, and orbital cutoff quality. The core electrons were treated as effective core potentials. Each cluster model was optimized by minimizing the energy by the DFT calculation. The oxygen binding energies were calculated for each three-fold hollow site on the surface of the resulting Pt cluster model. The O atom was always kept at a distance of 2.07 Å from the three neighboring Pt atoms without the geometry optimization.

**General methods.** XPS spectra were obtained using a spectrometer (Ulvac-Phi, ESCA1700R) with Mg K $\alpha$  radiation. For the XPS measurement, gold powder was deposited on a glassy carbon substrate (Tokai Carbon Co., Ltd.) as an internal standard with the cluster sample, and the Au 4f<sub>7/2</sub> (84.0 eV) peak was used to offset the electron binding energy.

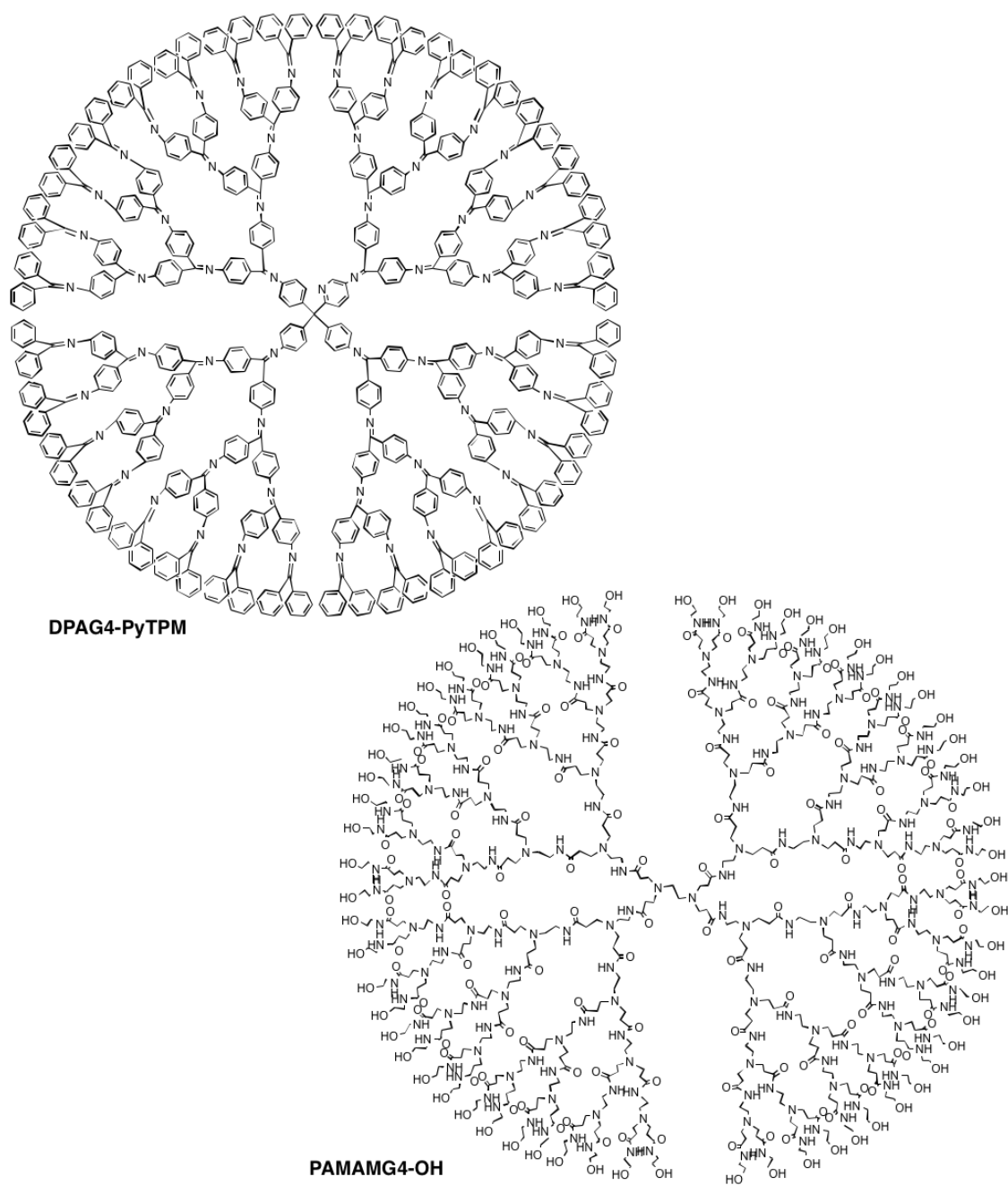


**Figure S1.** Structures of the dendrimers used in this study.

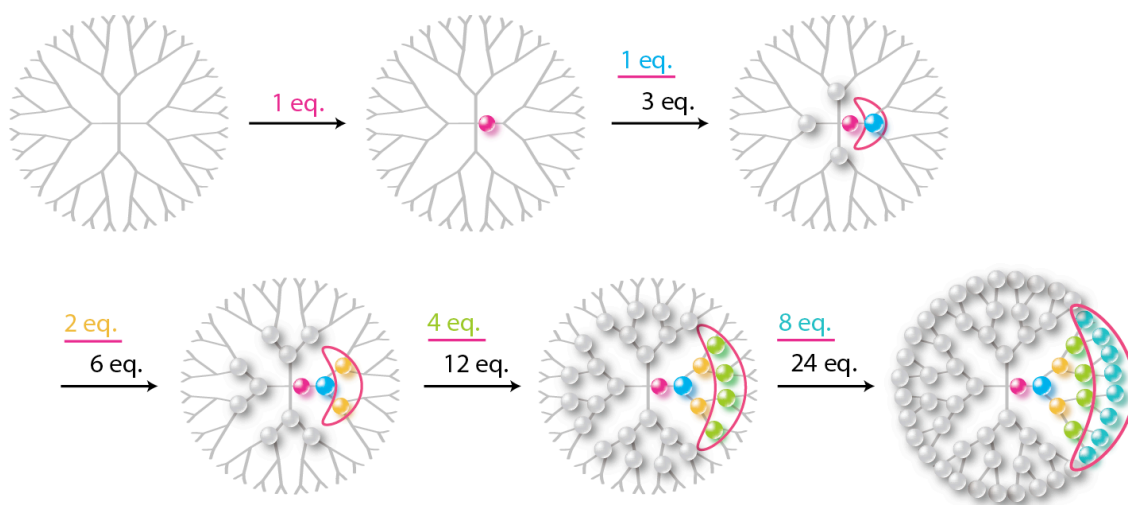


**Figure S2.** Schematic representation of the stepwise complexation to **DPAG4-PyTPM**.

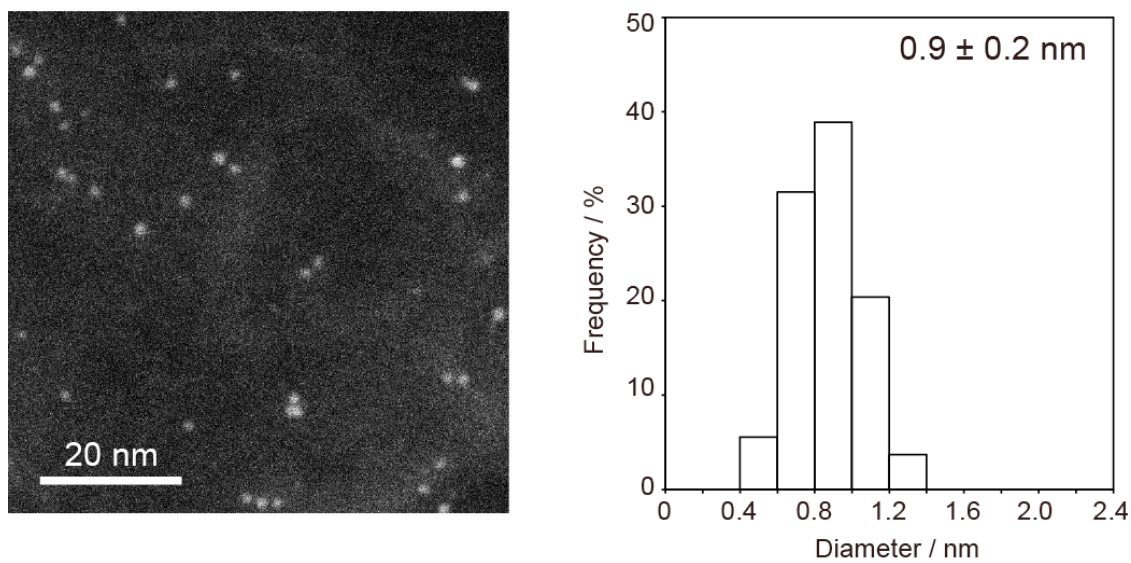


**Figure S3.** A HAADF-STEM image of Pt<sub>19</sub> with **PAMAMG4-OH** (left) and a histogram of the observed particle sizes (right).

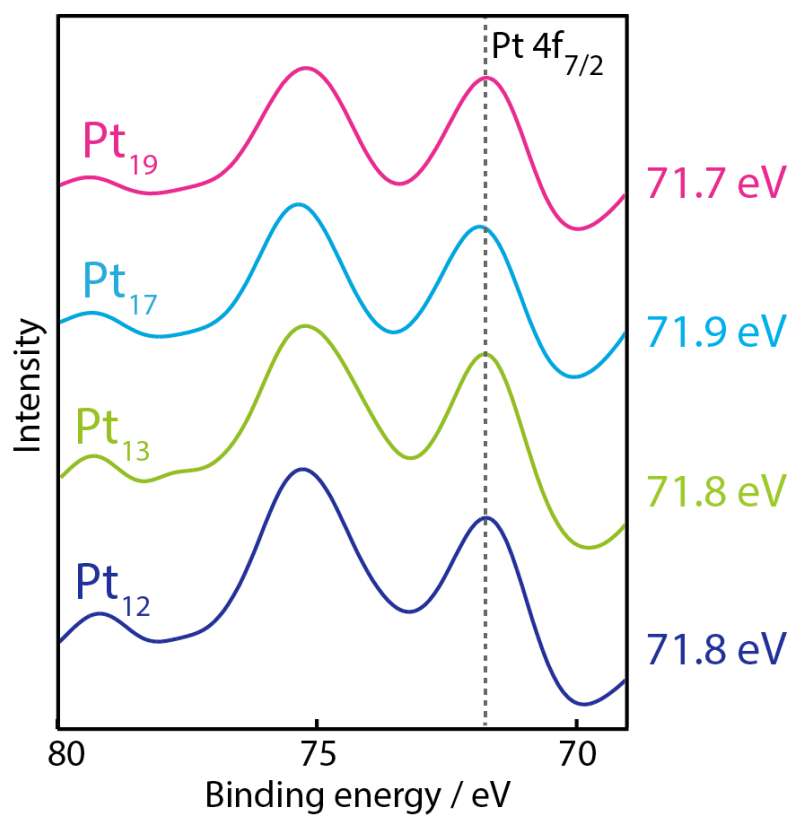


**Figure S4.** Pt 4f<sub>7/2</sub> X-ray photoelectron spectra of the clusters prepared with DPAG4-PyTPM or DPAG4-TPM.



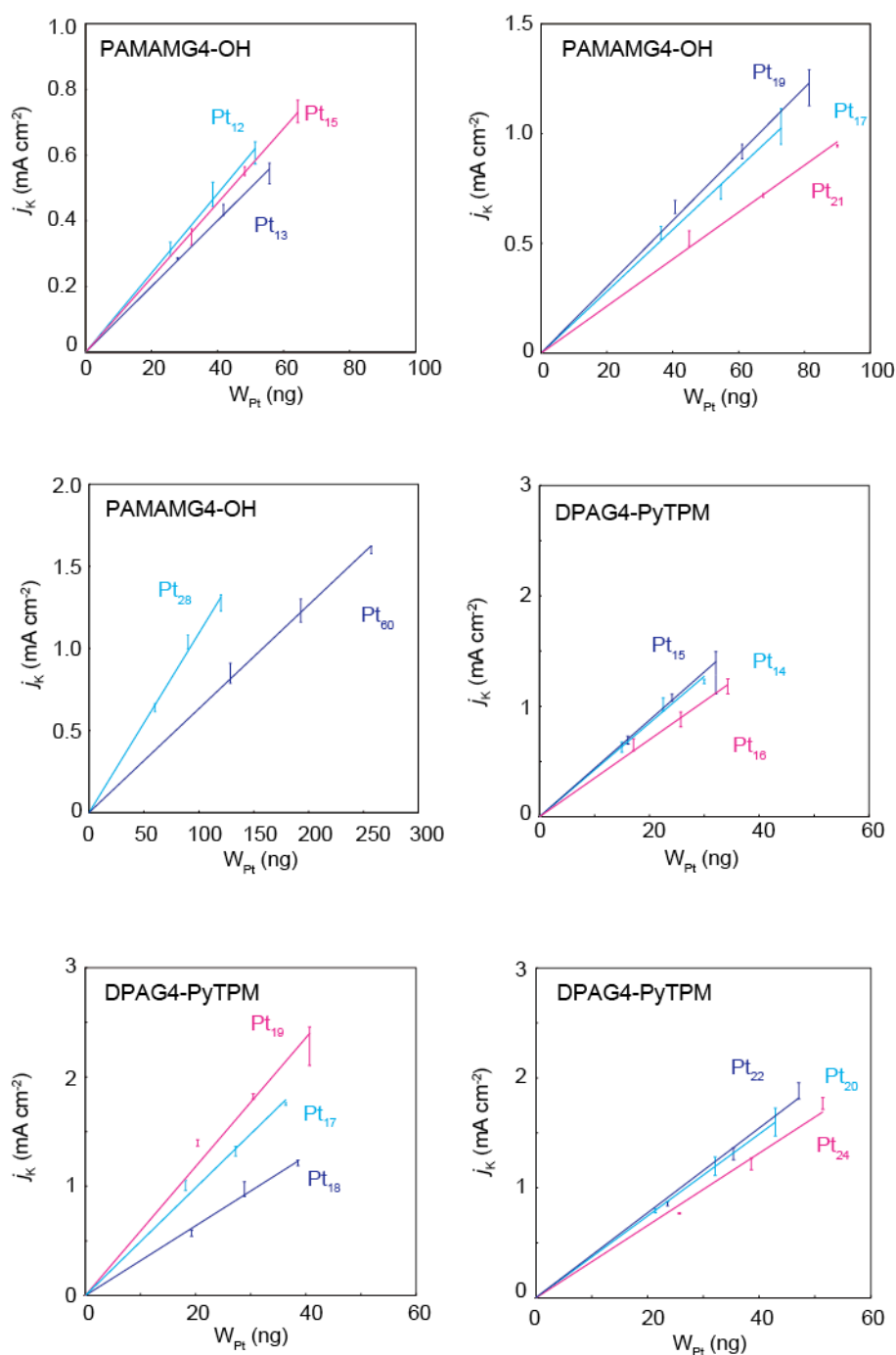


**Figure S5.** Kinetic current densities ( $j_K$ ) of the clusters prepared with both **PAMAMG4-OH** and **DPAG4-PyTPM**. The  $j_K$  values were calculated from the rotating disk voltammograms using the Koutecky-Levich equation for different amounts of clusters modified on the electrode.

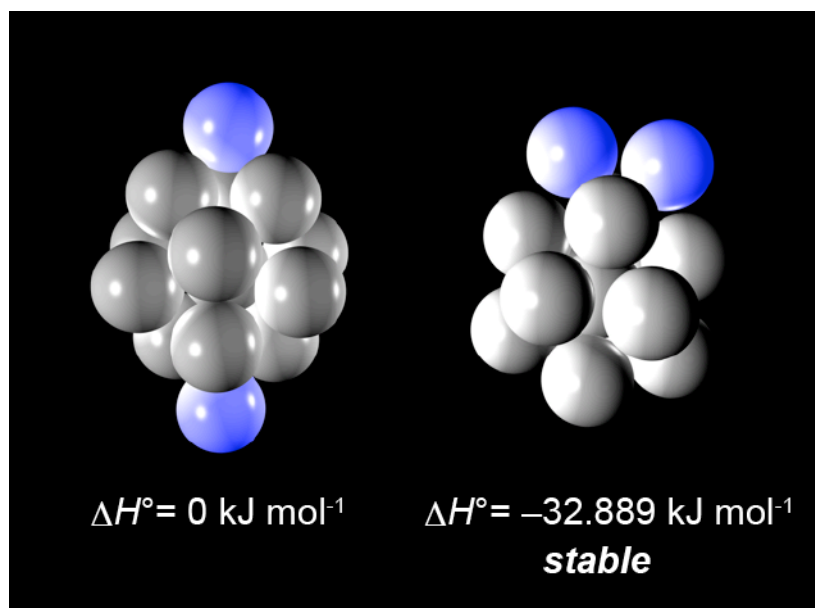


**Figure S6.** Possible cluster structures of Pt<sub>15</sub>. The DFT calculation suggested that the  $C_{2v}$  structure (right) is more stable.

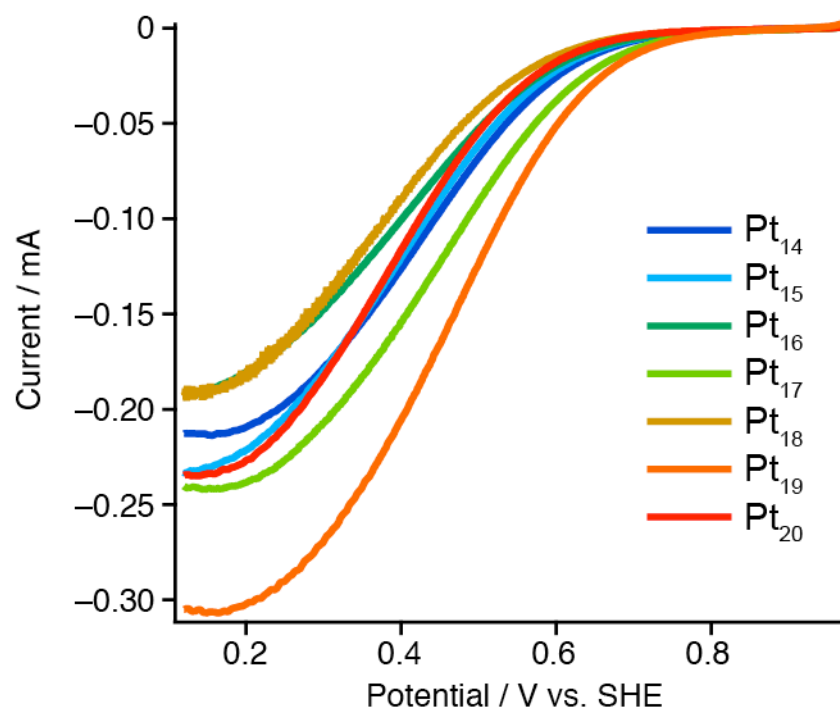


**Figure S7.** Rotating disk voltammograms (300 rpm) in an oxygen-saturating aqueous solution of HClO<sub>4</sub> (0.1 mol L<sup>-1</sup>) with modified electrodes with the platinum clusters (Pt<sub>14</sub> – Pt<sub>20</sub>). Very small amount of the clusters (ca. 30 ng) were directly modified onto a glassy carbon electrode in order to purely estimate the mass-activities without the oxygen migrations and the electron transport through a thick carbon film.

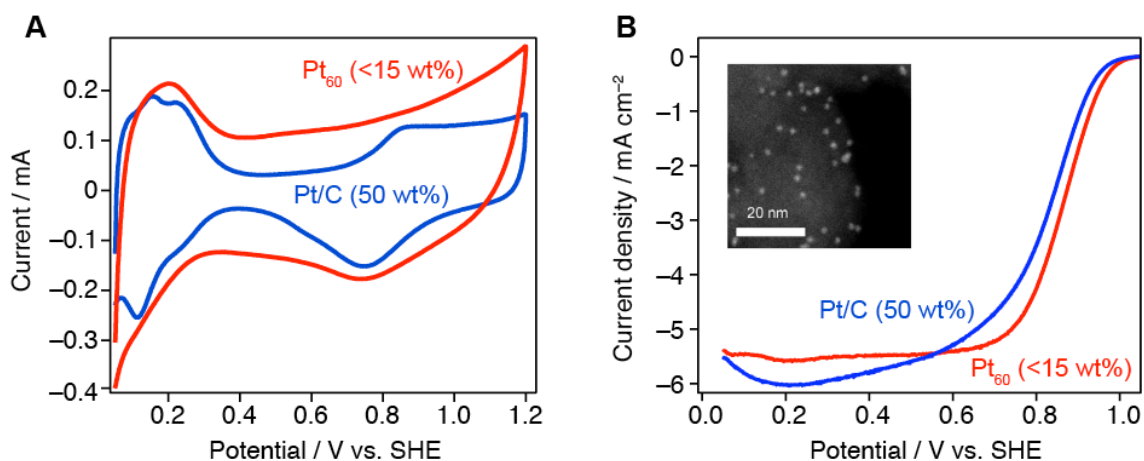


**Figure S8.** (A) Cyclic voltammograms of commercial Pt/C (50 wt% Pt) and Pt<sub>60</sub> (max. 15 wt% Pt) supported on a KetchenBlack EC® under an N<sub>2</sub>-saturating condition. (B) ORR polarization curves (1600 rpm) of the catalysts under an O<sub>2</sub>-saturating condition, and a HAADF-STEM image of the Pt<sub>60</sub> catalyst with the carbon support. The amounts of platinum on the glassy carbon electrode were 4.53 μg (Pt/C) and 4.24 μg (Pt<sub>60</sub>). Nafion® was coated on the electrode surface to facilitate the proton transfer. The measurements were carried out in an aqueous solution of HClO<sub>4</sub> (0.1 mol L<sup>-1</sup>) using a reversible hydrogen electrode (RHE) with a hydrogen reservoir.

**Table S1.** Curve fitting results of the EXAFS. These cluster samples were prepared with **DPAG4-PyTPM** or **DPAG4-TPM**.

sample	bond	$N$	$r / \text{\AA}$	$\Delta E_0 / \text{eV}$	$\Delta\sigma^2 / 10^{-3} \text{\AA}^2$	$R_f / \%$
Pt foil <sup>a</sup>	Pt-Pt	12	2.77	<i>n/a</i>	<i>n/a</i>	<i>n/a</i>
Pt <sub>12</sub>	Pt-Pt	$4.1 \pm 0.8$	$2.730 \pm 0.007$	$-7.1 \pm 2.7$	$2.64 \pm 0.08$	4.9
Pt <sub>13</sub>	Pt-Pt	$5.5 \pm 1.0$	$2.747 \pm 0.007$	$-3.0 \pm 2.5$	$3.29 \pm 0.06$	1.2
Pt <sub>17</sub>	Pt-Pt	$5.1 \pm 1.1$	$2.743 \pm 0.007$	$-5.5 \pm 2.9$	$1.44 \pm 0.10$	3.0
Pt <sub>19</sub>	Pt-Pt	$5.9 \pm 1.3$	$2.748 \pm 0.007$	$-4.1 \pm 2.8$	$2.03 \pm 0.10$	1.9
Pt/C <sup>b</sup>	Pt-Pt	$9.7 \pm 1.7$	$2.750 \pm 0.007$	$-3.8 \pm 2.3$	$4.14 \pm 0.06$	1.8

<sup>a</sup> Crystallographic data

<sup>b</sup> Commercially available platinum nanoparticle catalyst on carbon (TEC10E50E).

\* $N$ , coordination number;  $r$ , bond distance between absorber and backscatter atoms;  $\Delta\sigma^2$ , the Debye-Waller factor (DW), which is relative to the DW of the reference (Pt foil);  $\Delta E_0$ , the inner potential correction accounts for the difference in the inner potential between the sample and the reference;  $R_f$  ( $R$ -factor), a goodness of curve fit

\*\*Fourier transform and Fourier filtering region were limited where  $\Delta k = 3 \sim 16 \text{\AA}^{-1}$  and  $\Delta r = 1.964 \sim 3.007 \text{\AA}$ , respectively.

**Table S2.** The total number of unoccupied d-states per Pt atoms ( $(h_j)t,s$ ) calculated from the XANES data measured under *in-situ* electrochemical conditions. These clusters were prepared with **DPAG4-PyTPM**.

Potential	$(h_j)t,s$			
V vs. Ag/AgCl	Pt <sub>12</sub>	Pt <sub>13</sub>	Pt <sub>17</sub>	Pt <sub>19</sub>
0.00	0.364	0.354	0.356	0.355
0.65	0.365	0.367	0.369	0.367
1.00	0.450	0.474	0.439	0.479
1.40	0.526	0.519	0.503	0.551
0.00 (returned)	0.374	0.385	0.361	0.362

**Table S3.** Calculated oxygen binding energies to the 3-fold hollow sites of the possible clusters shown in Figure 4. Values in parentheses indicate the number of equivalent coordination sites in the cluster.

model	$\Delta E$ (eV) <sup>b</sup>
Pt <sub>15</sub>	-0.083(2), -0.124(4), -0.214(4), -0.235(2), -0.326(4), -0.382(2), -0.394(2), -0.402(4)
Pt <sub>17</sub>	0.146(4), 0.053(8), 0.041(8), -0.630(4), -0.673(4)
Pt <sub>19</sub>	0.092(6), 0.020(6), 0.004(6), -0.005(6), -0.122(6), -0.324(2)

## References

- [1] T. Imaoka, H. Kitazawa, W.-J. Chun, S. Omura, K. Albrecht, K. Yamamoto, *J. Am. Chem. Soc.* **2013**, *135*, 13089–3095.
- [2] H. Ye, R. M. Crooks, *J. Am. Chem. Soc.* **2005**, *127*, 4930.
- [3] K. Yamamoto, T. Imaoka, W.-J. Chun, O. Enoki, H. Katoh, M. Takenaga, A. Sonoi, *Nature Chem.* **2009**, *1*, 397.
- [4] B. Delley, *J. Chem. Phys.* **2000**, *113*, 7756.